GEOPHYSICAL RESEARCH LETTERS, VOL. 24, NO. 6, PAGES 643-646, MARCH 15, 1997

Temperature dependence of the collisional removal of $O_2(A\,^3\Sigma_u^+, \upsilon = 9)$ with O_2 and N_2

Eunsook S. Hwang and Richard A. Copeland

Aeronomy Program, Molecular Physics Laboratory, SRI International, Menlo Park, California

Abstract. The temperature dependence of the collisional removal of O_2 molecules in the $\upsilon = 9$ level of the $A^3\Sigma_u^+$ electronic state has been studied for the colliders O_2 and N_2, over the temperature range 150 to 300 K. In a cooled flow cell, the output of a pulsed dye laser excites the O_2 to the $\upsilon = 9$ level of the $A^3\Sigma_u^+$ state, and the output of a time-delayed second laser monitors the temporal evolution of this level via a resonance-enhanced ionization. We find the thermally averaged removal cross section for O_2 collisions is constant (~ 10 Å^2) between room temperature and 200 K, then increases rapidly with decreasing temperature, doubling by 150 K. In contrast, the N_2 cross section at 225 K is ~ 8% smaller and gradually increases to a value at 150 K that is ~ 60% larger than the room temperature value. The difference between the temperature dependence of the O_2 and N_2 collision cross section implies that the removal by oxygen becomes more important at the lower temperatures found in the mesosphere, but removal by N_2 still dominates.

Introduction

Ultraviolet and visible emissions from the Herzberg states ($A^3\Sigma_u^+$, $A'^3\Delta_u$, $c^1\Sigma_u^-$) of molecular oxygen are observed in the nightglow of the Earth [*Meriwether*, 1989] and Venus [*Fox*, 1986]. These electronic states of O_2 are generated in the upper atmosphere by the three body recombination of two oxygen atoms. Once formed, the excited O_2 can either radiate or undergo collisional relaxation. Because of the metastability of these states [*Huestis et al.*, 1994], collisional processes strongly influence the fluorescence intensity at the pressures and temperatures (150 - 250 K) of the emitting layer on Earth. The emissions from these states are used to monitor the properties and long- and short-term variability of the upper atmosphere from the ground or from satellites [*Murtagh*, 1995]. To understand the intensity and vibrational distribution of the Herzberg state emission, rate constants for collisional energy transfer with the major atmospheric species are required for atmospheric model input data [*Johnston and Broadfoot*, 1993]. Until recently, knowledge of the collision processes in these states was extremely limited. Over the last few years, two-laser, state-specific investigations in this laboratory have shown very rapid removal of O_2 molecules from the high vibrational levels in collisions with both O_2 and N_2 [*Copeland et al.*, 1996; *Knutsen et al.*, 1994]. This information, while crucial, cannot be used directly as input to the atmospheric models without additional assumptions on the temperature dependence of these rate constants. In the Earth's atmosphere, the emission occurs at altitudes where the temperature is significantly different from room temperature. Until this work, no measurements have been made on the collisional removal of these excited levels at the 150 to 225 K temperatures common in the region of the emission in the atmosphere. In this work, we measure the temperature dependence of the collisional removal of O_2 molecules in the $\upsilon = 9$ level of the $A^3\Sigma_u^+$ electronic state. A temperature range from 150 K to room temperature is examined, spanning the temperatures found in the oxygen nightglow layer. Although the $\upsilon = 9$ level is slightly higher in energy than the levels at the peak of the vibrational distribution observed in the atmosphere ($3 \le \upsilon \le 8$) [*Meriwether*, 1989], the $\upsilon = 9$ temperature dependence should be similar to those more populated vibrational levels. Experimental verification of this assumption is under way.

The only temperature dependent energy transfer information on excited electronic states in O_2 is for the $a^1\Delta_g$ and the $b^1\Sigma_g^+$ states in the $\upsilon = 0$ levels [*Billington and Borrell*, 1986; *Kohse-Höinghaus and Stuhl*, 1980]. For the $b^1\Sigma_g^+$ electronic state, where N_2 removal dominates over O_2 removal for the primary atmospheric species, the rate constant for N_2 is independent of temperature from 203 to 349 K (i.e., the thermally averaged collision cross section increases slightly with decreasing temperature) [*Kohse-Höinghaus and Stuhl*, 1980]. For the $a^1\Delta_g$ electronic state, where O_2 removal dominates over N_2 removal, the rate constant for O_2 decreases by more than a factor of four going from room temperature to 100 K [*Billington and Borrell*, 1986]. These processes are about 2×10^4 and 2×10^7 times slower for the $b^1\Sigma_g^+$ and $a^1\Delta_g$ states, respectively, than the removal of the high vibrational levels of the Herzberg states and, because of this, may show significantly different dependence on temperature. Clearly, the only way to know for certain what the rate constants will be at the relevant atmospheric temperatures is to make the measurement directly for all colliders where the information is important. Room temperature results indicate that the removal rate constants for N_2 and O_2 are comparable, so both colliders must be examined.

Experimental Approach and Results

The experimental approach has been described in detail previously [*Knutsen et al.*, 1994]. Herein, we will briefly review this information and focus on the aspects of the approach unique to this study of the temperature dependence. A two-chamber, independently pumped flow cell is used for this study. The inner observation chamber is connected to a vacuum-isolated copper flow tube approximately 20 cm long that is in close contact with a reservoir containing either dry-ice/acetone or liquid nitrogen. The outer chamber is evacuated by a separate mechanical pump to minimize thermal transport

Paper number 97GL00547.
0094-8534/97/97GL-00547$05.00

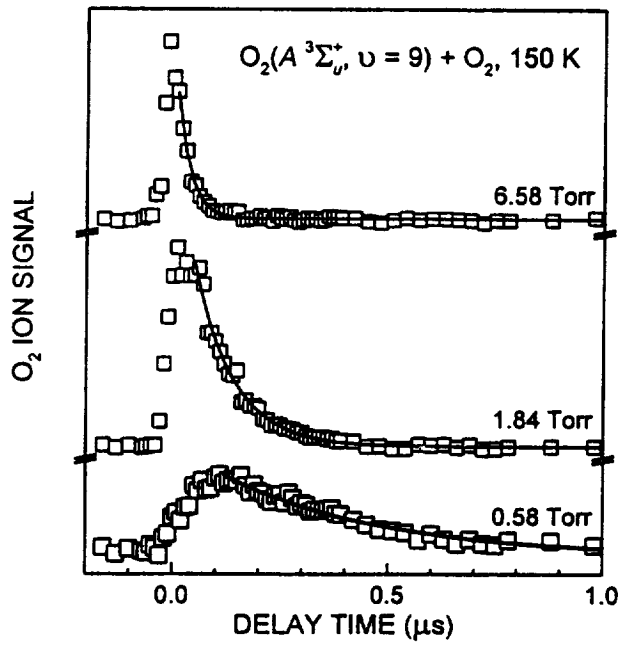

Figure 1. Plots of the $O_2(A^3\Sigma_u^+, \upsilon = 9)$ ion signal versus delay time in pure O_2 at different pressures. The open squares are the experimental data points and the solid lines are the best-fit single exponential to the data. The slow rise of the signal, as clearly seen in the 0.58-Torr data (lowest curve), is due to rotational equilibration into the probed rotational level.

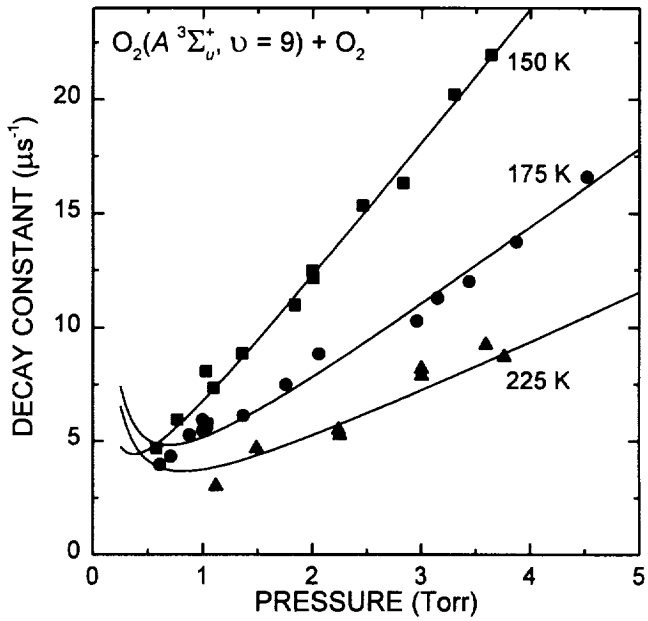

Figure 2. Plots of decay constant versus pressure for $O_2(A^3\Sigma_u^+, \upsilon = 9)$ colliding with O_2 at various temperatures. The solid lines represent the best nonlinear least-squares fit to the data using Equation 1. Diffusion contributes significantly to the decay constant only at lower pressures and generates the upturn in the fits.

from the cooled inner cell, thereby isolating the inner cell. In this two-laser experiment, the frequency-doubled output of a focused (50-cm focal length lens) excimer-pumped dye laser excites the ground state O_2 molecules to the $\upsilon = 9$ level of the $A^3\Sigma_u^+$ state. We select the $\upsilon = 9$ level for an initial investigation because of the large signals observed in the room temperature investigation of this vibrational level in our laboratory [*Knutsen et al.*, 1994]. We excite to the N = J = 9 rotational level for temperatures from room temperature down to 225 K, and the N = J = 5 level for lower temperatures [*Coquart and Ramsay*, 1986]. The wavelengths for excitation are $\lambda = 246.75$ nm and 246.46 nm, respectively. The 290.1-nm light from the second laser, a frequency-doubled, focused (50-cm focal length lens), Nd:YAG-pumped dye laser, monitors the $\upsilon = 9$ level via resonant-enhanced ionization through transitions tentatively assigned to ionization through the $5^3\Pi_g$ valence state and an overlapping absorption through the $\upsilon = 5$ level of the $C^3\Pi_g$ state [*Knutsen et al.*, 1994]. A thin wire electrode is biased to voltages between -20 to -90 V for positive ion collection. The temporal evolution of the signal is obtained by scanning the time delay between the two laser pulses. Once excited, O_2 molecules undergo rapid rotational equilibration within the prepared $\upsilon = 9$ vibrational level. As described in the room temperature study [*Knutsen et al.*, 1994], rotational level effects are minimized by monitoring rotational levels lower in energy than those initially excited. A feature due to overlapping ionizations of N = 1 and 3 near 290.1 nm is used in all the measurements in this work.

A 0.01-in. diameter copper-constantan thermocouple monitors the temperature of the gas near the overlapping laser beams (~ 4 mm away). To verify that the thermocouple measurement agrees with the gas temperature in the beam overlap region, we seed a small amount of NO into the system under our typical flow conditions. The frequency-doubled output of the dye laser near 211.05 nm excites NO to the $\upsilon = 2$ level of the $B^2\Pi$ state, and fluorescence from the $B^2\Pi$ state is monitored at right angles through a 256 ± 5 nm filter with a photomultiplier tube (Hamamatsu R666-10). The laser-induced fluorescence signal is amplified, averaged with a gated integrator (SRS) and recorded with a computer. The temperature is deduced by comparing the experimental ratio of the integrated area of two adjacent rotational lines, $P_2(7.5)$ and $R_1(16.5)$, with a value calculated from the DIATOM computer program [*Huestis*, 1994]. This ratio changes from 0.70 at 300 K to 0.21 at 150 K. At approximately 160 K, the thermocouple and the NO rotational temperature agree within +/- 8 K (2-σ). Over the entire temperature range, we assign either a ± 10 K or ± 11 K temperature uncertainty depending on the variation of the thermocouple value during the measurement.

Typical experimental data at three pressures of pure O_2 are shown in Figure 1. The displayed data is the subtraction of 70 laser shots (10-Hz repetition rate) on resonance and off resonance at each delay position. As the pressure increases, the signal both rises and falls more rapidly. The rise of the signal is clearly seen in the 0.58-Torr data at the bottom of the figure. The rise is due to rotational equilibration into the probed rotational level from the excited rotational level and the fall is the removal out of the equilibrated vibrational level. To obtain a signal decay constant for the experimental data, we fit the signal to a single exponential from approximately 50 percent of the peak to long delay times. The decay constant is the sum of all removal processes from the prepared vibrational state and includes collisional energy transfer, reaction, radiation, and diffusion/flight out of the

Table 1. O_2 ($A^3\Sigma_u^+$, $\upsilon = 9$) Collisional Removal Rate Constants, Thermally Averaged Cross Sections, and Effective Diffusion Rate Constants[a]

Collider	T (K)	k (10^{-11} cm^3 s^{-1})	σ (Å^2)	D (μs^{-1} Torr)
O_2	298 ± 10	6.38 ± 0.44	10.2 ± 0.6	2.10 ± 0.74
	257 ± 11	6.39 ± 0.36	11.0 ± 0.5	2.42 ± 0.54
	225 ± 10	5.24 ± 0.32	9.6 ± 0.4	1.51 ± 1.36
	198 ± 11	5.70 ± 0.45	11.1 ± 0.7	1.64 ± 0.78
	175 ± 11	6.34 ± 0.47	13.2 ± 0.7	1.65 ± 0.40
	161 ± 11	7.91 ± 0.72	17.1 ± 1.2	0.50 ± 0.42
	150 ± 10	9.22 ± 0.75	20.7 ± 1.0	0.82 ± 0.50
N_2	250 ± 11	4.43 ± 0.50	7.4 ± 0.7	—
	225 ± 10	3.42 ± 0.28	6.1 ± 0.4	—
	200 ± 11	5.13 ± 0.61	9.6 ± 1.0	—
	175 ± 11	4.55 ± 0.48	9.1 ± 0.8	—
	150 ± 10	4.81 ± 0.43	10.4 ± 0.6	—

[a] All error estimates are two standard deviations.

observation region. Typical single exponential fits are displayed in Figure 1 as the solid lines. We begin fitting at 50% to eliminate any complications from rotational filling of the probed rotational levels, but the curves fit well to much shorter delay times as shown in Figure 1. At each temperature we vary the pressure of the O_2 or, in the case of the N_2 measurements, maintain the pressure of O_2 constant and vary the N_2 partial pressure. For the mixed gas measurements, mass flowmeters are used in conjunction with the total pressure to obtain the partial pressure of O_2 and N_2.

At the lowest pressures, diffusion/flight out of the beam overlap region can contribute to the signal decay. We approximate the diffusion correction with the following simple equation, and since the diffusion correction has only a small effect on the extracted total signal decay constants this approximation is adequate [*Knutsen et al.*, 1994]. The signal decay constant, τ^{-1}, is approximated by the following equation:

$$\tau^{-1} = k_{O_2}P_{O_2} + k_{N_2}P_{N_2} + D/P \qquad (1)$$

where P is the total pressure in the cell, P_x is the partial pressure of species x, k_x is the removal rate constant for species x, and D is an effective diffusion rate for the specific experimental conditions. Figure 2 shows a plot of decay constants versus pressure at various temperatures for removal of the $\upsilon = 9$ level in the $A^3\Sigma_u^+$ state with only O_2 in the cell. The rate constants for oxygen removal are obtained via nonlinear fits to Equation 1 and are shown by the solid lines in Figure 2. The results of these fits are collected in Table 1. Neglecting diffusion in the worst case only decreases the extracted rate constant by 20% and would decrease the quality of the fit by forcing the solid lines in Figure 2 through the origin. The thermally averaged cross section, σ_x, is obtained from the following equation:

$$k_x = \langle v \rangle \sigma_x \qquad (2)$$

where $\langle v \rangle$ is the average relative collision velocity at the temperature of the measurement. The thermally averaged cross sections remove the trivial velocity dependent change in the collision frequency so that straightforward comparisons of efficiencies at different temperatures can be made. The error estimates in Table 1 are, in the case of the diffusion rate, those obtained from the nonlinear fit. For the rate constant the error estimates are the fit results convolved with the temperature uncertainty, while for the cross section the error estimates are the fit uncertainty combined with the $T^{1/2}$ uncertainty in the conversion.

To obtain rate constants for the removal of O_2 ($A^3\Sigma_u^+$, $\upsilon = 9$) with N_2 as a collider, we measure the decay constant with the N_2 partial pressure varied while the O_2 partial pressure is kept constant. For the 200-300 K range, we keep the O_2 pressure at 3 Torr, while below 200 K the O_2 pressure is 1 Torr. This change is required because of the increase in the removal by O_2 at low temperatures. Rate constants are extracted from nonlinear fits to Equation 1, with k_{O_2} and D fixed to the values obtained from the O_2 collider. Approximating D for N_2 to the oxygen value has little effect, given the similarity between N_2 and O_2. The N_2 rate constants and thermally averaged collision cross sections are given in Table 1. If k_{O_2} and D are varied within their 2-σ uncertainties, the extracted rate constant only decreases by 20% in the worst case. Error estimates are a combination of the temperature error and the uncertainty in the nonlinear fits. The errors are larger and the data are more scattered than in the corresponding O_2 data.

Discussion

Figure 3 displays the temperature dependence of the thermally averaged collision cross section for removal of the $\upsilon = 9$ level of $A^3\Sigma_u^+$ state by the colliders O_2 and N_2. At room temperature, agreement with the previous measurements from this laboratory [*Knutsen et al.*, 1994] for O_2 is excellent. For O_2 [Figure 3(b)], the thermally averaged cross

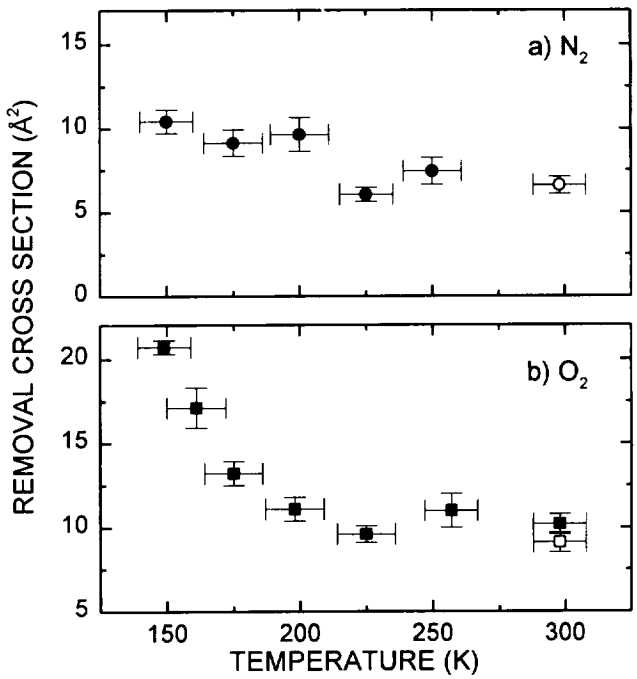

Figure 3. Plots of thermally averaged cross section versus temperature for O_2($A^3\Sigma_u^+$, $\upsilon = 9$) colliding with O_2 and N_2. The open symbols are the values reported previously [*Knutsen et al.*, 1994] and the solid symbols are the results of this work.

section does not change significantly until 175 K, where a statistically significant increase is observed, and by 150 K, the cross section has doubled. For N_2 [Figure 3(a)], the temperature effects are less dramatic. The cross section does not change significantly until 200 K, and the values seem to show only a small increase with decreasing temperature. The room temperature value from previous work in this laboratory [*Knutsen et al.*, 1994] is included in Figure 3 to complete the temperature range. Because of this difference in the temperature dependence of the cross section for O_2 and N_2, as the temperature decreases in the mesosphere the $A^3\Sigma_u^+$ state removal by O_2 will become more important. However, even with the factor of two difference in the cross sections at 150 K, N_2 removal will still dominate given its natural abundance in the atmosphere.

The temperature dependence of $A^3\Sigma_u^+$ state removal can be compared with those observed at low temperatures for the $a^1\Delta_g$ and $b^1\Sigma_g^+$ states of O_2. The factor of four decrease in the rate constant observed for removal of the $a^1\Delta_g$ state with O_2 from room temperature to 100 K is very different from what is observed here [*Billington and Borrell*, 1986]. For our significantly faster process, a different mechanism must apply. Typically, processes dominated by short-range interactions show a decrease in the rate constant with decreasing temperature, while processes dominated by long-range interactions show an increase. A comparison with the $b^1\Sigma_g^+$ removal shows similar behavior to that observed here; the rate constant for N_2 does not change significantly in the temperature range 200 to 300 K (see Table 1) [*Kohse-Höinghaus and Stuhl*, 1980]. In both cases, because the rate constant does not change, the thermally averaged cross section must increase with decreasing temperature. In the earlier study on the $b^1\Sigma_g^+$ state, temperatures below 200 K were not measured, so the low-temperature behavior is unknown. Our results on $O_2(A^3\Sigma_u^+)$ colliding with O_2 is one of the few combinations showing such a dramatic increase over such a small temperature range.

Comparison with a few other diatomic molecules in electronically excited states is instructive. OH ($A^2\Sigma^+$) state removal shows a large increase with decreasing temperatures which has been attributed to the dominant role of attractive forces at low temperature [*Copeland and Crosley*, 1986]. This increase is observed throughout the temperature range examined here. The large dipole moment of OH contributing to the long-range attractive forces is thought to be the cause of this temperature dependence. For NO, a molecule with a smaller dipole moment, the removal cross sections for collision with O_2 are constant in the $v = 0$ levels of the $A^2\Sigma^+$ and $B^2\Pi$ states above room temperature [*Raiche and Crosley*, 1990]. The $A^2\Sigma^+$ cross section increases slightly (~18%) as the temperature is lowered from 300 K to 215 K [*Zhang and Crosley*, 1995]. The surprising aspect for the $O_2(A^3\Sigma_u^+)$ state removal cross section, which has no dipole moment in contrast to OH and NO molecules, is the rapid increase below 200 K for O_2 collider. Clearly, removal is enhanced due to the longer duration of the collision, but whether it is caused by one pathway among several competing pathways requires further investigation.

To date, we have only studied the temperature dependence in one vibrational level of one of the three Herzberg states. More measurements are needed to model the relaxation process in the entire manifold of states. The large changes in temperature seen with O_2 might be due to a change in mechanism, which is also under investigation.

Acknowledgments. This work is supported by the National Aeronautics and Space Administration, Space Physics Division (NASW-4440). We thank David Huestis, Mark Dyer, and Tom Slanger for their helpful contributions.

References

Billington, A. P., and P. Borrell, The low-temperature quenching of singlet molecular oxygen [$O_2(a^1\Delta_g)$], *J. Chem. Soc. Faraday Trans. 2, 82*, 963-970, 1986.

Copeland, R. A., and D. R. Crosley, Temperature dependent electronic quenching of OH($A^2\Sigma^+$, $v = 0$) between 230 and 310 K, *J. Chem. Phys., 84*, 3099-3105, 1986.

Copeland, R. A., K. Knutsen, M. E. Onishi, and T. Yalçin, Collisional removal of $O_2(c^1\Sigma_u^-$, $v = 9)$ by O_2, N_2, and He, *J. Chem. Phys., 105*, 10349-10355, 1996.

Coquart, B., and D. A. Ramsay, High-resolution studies of the near-ultraviolet bands of oxygen: III: The $A^3\Delta_u - X^3\Sigma_g^-$, system, *Can. J. Phys., 64*, 726-732, 1986.

Fox, J. L., Models for aurora and airglow emissions from other planetary atmospheres, *Can. J. Phys., 64*, 1631-1656, 1986.

Huestis, D. L., DIATOM Spectral Simulation Computer Program, SRI International, Menlo Park, Calif., 1994.

Huestis, D. L., R. A. Copeland, K. Knutsen, T. G. Slanger, R. T. Jongma, M. G. H. Boogaarts, and G. Meijer, Branch intensities and oscillator strengths for the Herzberg absorption systems in oxygen, *Can. J. Phys., 72*, 1109-1121, 1994.

Johnston, J. E., and A. L. Broadfoot, Midlatitude observations of the night airglow: Implications to quenching near the mesopause, *J. Geophys. Res., 98*, 21593-21603, 1993.

Knutsen, K., M. J. Dyer, and R. A. Copeland, Laser double-resonance study of the collisional removal of $O_2(A^3\Sigma_u^+$, $v = 6, 7, 9)$ with O_2, N_2, CO_2, Ar, and He, *J. Chem. Phys., 101*, 7415-7422, 1994.

Kohse-Höinghaus, K., and F. Stuhl, H_2-laser photochemical study of the temperature dependent quenching of $O_2(b^1\Sigma_g^+)$, *J. Chem. Phys., 72*, 3720-3726, 1980.

Meriwether, J. W., Jr., A review of the photochemistry of selected nightglow emissions from the mesopause, *J. Geophys. Res., 94*, 14629-14646, 1989.

Murtagh, D. P., The State of O_2 in the Mesopause Region, in *The Upper Mesosphere and Lower Thermosphere: A Review of Experiment and Theory*, edited by R. M. Johnson and T. L. Killeen, pp. 243-249, American Geophysical Union, Washington, DC, 1995.

Raiche, G. A., and D. R. Crosley, Temperature dependent quenching of the $A^2\Sigma^+$ and $B^2\Pi$ states of NO, *J. Chem. Phys., 92*, 5211-5217, 1990.

Zhang, R., and D. R. Crosley, Temperature dependent quenching of $A^2\Sigma^+$ NO between 215 and 300 K, *J. Chem. Phys., 102*, 7418-7424, 1995.

E. S. Hwang and R. A. Copeland, SRI International, 333 Ravenswood Avenue, Menlo Park, CA 94025. (e-mail: hwang_es@mplvax.sri.com; rich@mplvax.sri.com)

(Received October 22, 1996; revised February 20, 1997; accepted February 24, 1997.)